Vaccine 36 (2018) 1016–1023

Contents lists available at ScienceDirect

Vaccine

journal homepage: www.elsevier.com/locate/vaccine

A single dose polyanhydride-based vaccine platform promotes and maintains anti-GnRH antibody titers

Robert G. Schaut [a,1,2], Matthew T. Brewer [a,1], Jesse M. Hostetter [a], Kriscelle Mendoza [a,3], Julia E. Vela-Ramirez [b,4], Sean M. Kelly [b], John K. Jackman [c], Giuseppe Dell'Anna [d], Joan M. Howard [e], Balaji Narasimhan [b,f], Wen Zhou [g], Douglas E. Jones [a,f,*]

[a] Department of Veterinary Pathology, Iowa State University, Ames, IA 50011, USA
[b] Department of Chemical and Biological Engineering, Iowa State University, Ames, IA 50011, USA
[c] Department of Industrial and Manufacturing Systems Engineering, Iowa State University, Ames, IA 50011, USA
[d] Laboratory Animal Resources, Iowa State University, Ames, IA 50011, USA
[e] Department of Veterinary Clinical Sciences, Iowa State University, Ames, IA 50011, USA
[f] Nanovaccine Institute, Iowa State University, Ames, IA 50011, USA
[g] Department of Statistics, Colorado State University, Fort Collins, CO 80523, USA

ARTICLE INFO

Article history:
Received 1 September 2017
Received in revised form 8 December 2017
Accepted 18 December 2017

Keywords:
GnRH
Vaccine
Immunocastration
Antibodies
Implant
Single-dose

ABSTRACT

Traditionally, vaccination strategies require an initial priming vaccination followed by an antigen boost to generate adequate immunity. Here we describe vaccination against a self-peptide for reproductive sterilization utilizing a three-stage vaccine platform consisting of gonadotropin releasing hormone multiple antigenic peptide (GnRH-MAP) as a soluble injection coupled with subcutaneous administration of polyanhydride-immobilized GnRH-MAP and a cyto-exclusive implant containing GnRH-MAP dendrimer-loaded polyanhydride. This strategy generated and maintained cell-mediated and humoral immunity for up to 41 weeks after a single vaccination in mice with enhanced antibody avidity over time. All intact implants had a grossly visible tissue interface with neovascularization and lymphocytic aggregates. Despite detectable immunity, sterility was not achieved and the immune response did not lead to azoospermia in male mice nor prevent estrus and ovulation in female mice. However, the vaccine delivery device is tunable and the immunogen, adjuvants and release rates can all be modified to enhance immunity. This technology has broad implications for the development of long-term vaccination schemes.

1. Introduction

An optimal immune response to vaccination includes the generation and maintenance of protective levels of antibodies or cell-mediated immunity. However, both of these responses rarely occur after a single administration of a vaccine. The phenomenon of concomitant immunity wherein the host generates and maintains protective immunity after an infection illustrates that there are mechanisms by which long-term immunity could be initiated and maintained after a single vaccination [1]. For example, resolved *Leishmania major* infection is a dynamic relationship between surviving and dying parasites in the lesion and the resulting concomitant immunity is dependent upon short-lived non-proliferating $CD4^+$ T cells maintained by persistent antigen [2,3]. Development of a single-dose vaccine platform that mimics concomitant immunity, which could be adapted to different immunogens and adjuvants, would be a significant advance towards generating long-lasting protective vaccine responses.

An excellent model for such a platform are immunocastration vaccines targeting gonadotropin releasing hormone (GnRH), a 10 amino acid peptide hormone conserved across many species that is essential for sperm production in males and ovulation in females [4]. Maintaining effective levels of anti-GnRH antibodies are critical for effective long-term immunocontraception [5]. Some impor-

* Corresponding author at: Department of Veterinary Pathology, 2750 Vet Path, Vet Med Building, Ames, IA 50010, USA.
E-mail address: jonesdou@iastate.edu (D.E. Jones).
[1] These authors contributed equally to this work.
[2] Current address: National Animal Disease Center, 1920 Dayton Ave, Ames, IA 50010, USA.
[3] Current address: Louisiana State University School of Veterinary Medicine, Skip Bertman Dr., Baton Rouge, LA 70803, USA.
[4] Current address: University of Texas at Austin, Department of Biomedical Engineering, 107 W Dean Keeton St, Austin, TX 78712, USA.

https://doi.org/10.1016/j.vaccine.2017.12.050
0264-410X/

tant successes have been achieved with GnRH vaccines, such as Improvac™ for pigs, Equity™ for horses, Bopriva™ for cattle and Gonacon™. All of these formulations use GnRH linked to various carrier proteins with different adjuvants. Gonacon™ is single administration product registered for use in wildlife and feral horses that has demonstrated durable long-term immunocastration. Notably, dogs and male cats respond suboptimally to Gonacon™ and there remains a need to develop a multi-year single administration vaccine for immunocastration that could be tuned by adjusting the antigen, adjuvant and release rates to optimize the immune response in multiple species [6–9].

Polyanhydrides have been studied extensively and are known to be effective as a biocompatible micro- and nano-vaccine delivery platform that enhances immunity while protecting the immunogen in a surface eroding hydrophobic solid monolith. The rate of antigen release can be tuned by altering the degradation characteristics of the PA chemistry and/or the surface area of the PA exposed to hydrolysis [10–14]. The present study consisted of polyanhydride copolymers with a molar composition of 20% 1,8-bis(*p*-carboxyphenoxy)-3,6-dioxaoctane (CPTEG) and 80% 1,6-bis (*p*-carboxyphenoxy)hexane (CPH) (i.e., 20:80 CPTEG:CPH) due to its ability to stabilize entrapped proteins and the slow surface erosion characteristics of CPH-rich chemistries [10,15]. Additionally, polymer chemistry can be used to modulate immune responses. In the case of copolymers, this is typically achieved by varying the copolymer composition. It has been shown that copolymer composition can alter nanoparticle persistence and therefore the bioavailability of antigen over time [16]. It has also been previously demonstrated with polyanhydride-based nanovaccine formulations that the chemistry of the carrier resulted in differential antibody titer, avidity, and IgG subclass switching in immunized animals [17,18]. In another example, Haughney et al. reported that varying copolymer chemistry altered the persistence of polyanhydride nanoparticles as well as the kinetics and maturation of the B cell response, including antibody titer, avidity, and specificity to immunodominant linear epitopes of the target antigen [19].

In this study the vaccine platform has 3 stages, (1) an injection of soluble GnRH-Multiple Antigenic Peptide (MAP) linked to Blue Protein (BP) with alum to prime the immune system and initiate antibody-mediated immunity, (2) a pressed solid rod of PA that degrades at all surfaces over a timeframe compatible with a boosting immunization that releases GnRH-MAP and MPLA adjuvant to support a $CD4^+$ T helper cell response [20], and (3) long-term vaccine release from a PVDF membrane-capped cytoexclusive implant that encases a PA rod containing adjuvant free GnRH-MAP linked by polyethylene glycol dendrimers. In the implant PA degradation is limited to one surface and a diffusion barrier of collagen is placed above the vaccine depot for theoretical passive immunoregulation of antigen release by immune-complex deposition. We hypothesize that this design will promote extended immunity without multiple injections [21–25]. The aim of the current study was to assess gross and microscopic tissue changes associated with the vaccine platform, determine if such a vaccine platform could generate and maintain immunity, as well as assess the histopathology of reproductive tissue post-vaccination.

2. Materials and methods

2.1. Antigen Synthesis, formulation and adjuvants

GnRH was synthesized as an 8-subunit MAP (Pyr-HWSYGLRPGQHWSYGLRPG) as described by Beekman et al. [26] or as a GnRH-MAP linked to an 8 arm polyethelyne glycolated 40 K maleimide dendrimer (BioSynthesis, Lewisville, TX). Purity was validated via HPLC by the manufacturer and greater than 50%.

For soluble vaccine formulations, Blue Carrier™ Protein (BP) (Thermo Scientific) was coupled to GnRH-MAP via 1-Ethyl-3-(3-dimethylaminopropyl)carbomide (EDC) crosslinking following manufacturers recommendations [27]. GnRH-MAP-BP was washed with sterile phosphate buffered saline (PBS) via centrifuge purification with 20 kDa columns (Thermo Scientific). Successful crosslinking was confirmed via western blot analysis.

2.2. Soluble antigen formulation

The soluble vaccine was comprised of either 300 μg GnRH-MAP-BP (treatment) or sterile PBS (control) with 2 mg Alum (Imject® Alum, Thermo Scientific) in a volume of 100 μL.

2.3. Polyanhydride formulation

20:80 CPTEG:CPH copolymers were synthesized using melt polycondensation as previously described [10]. The number-average molecular weight and molar composition was quantified using ^{1}H NMR (DXR 500), specifically by end group analysis. The 20:80 CPTEG:CPH copolymers synthesized had a molecular weight of 5800 Da with a polydispersity index (PDI) of 1.5 and 21,000 Da with a PDI of 1.4, respectively.

2.4. Rod design

Polyanhydride rod design and synthesis is previously described [25] using 208 mg PA, 100 μg of Monophosphoryl Lipid A (MPLA) derived from *Salmonella minnesota* R595 (InvivoGen, San Diego, CA) (treatment) with or without 300 μg of GnRH-MAP. The estimated time for degradation from all surfaces is three months or 3.18 μg of GnRH-MAP released per day [28]. Dried mixtures of vaccine, PA, and MPLA were pressed in custom made mold under 2 metric tons pressure using a Carver press.

2.5. Implant design

The ultra high molecular weight polyethylene (UHMW-PE) implant has been described previously [25]. The implant is 20 mm long with an internal diameter of 4 mm with a volume of 206 μL and capped with a 0.65 μm pore PVDF membrane (EMD Millipore 3P DVPP00010 Durapor). To conserve GnRH-MAP dendrimer antigen, 70 mg of PA containing 450 μg of dendrimer was pressed as above and placed on top of pressed 70 mg of antigen-free PA resulting in a 140 mg PA insert with the antigen containing PA positioned towards the PVDF membrane. The estimated time to degradation from a single exposed surface with a diameter of 0.4 cm and depth of 1 cm is ca. 38 months or 0.794 μg of vaccine released per day [28]. For control group 7 (Fig. 1B) the implant contained 140 mg of antigen-free polyanhydride. The PA was then layered with approximately 100 μL of 0.5% type 1 bovine collagen (PureCol® EZ Gel, Advanced BioMatrix, San Diego, CA) and crosslinked as previously described [29]. The cap was then fixed with n-butyl cyanoacrylate (Vetbond™, 3 M St. Paul, MN) and stored in PBS at 4 °C until use.

2.6. Animals

C3HeB/FeJ mice were purchased from Jackson Labs (Bar Harbor, ME). All experiments with animals were in accordance with the National Institutes of Health Guide for the Care and Use of Laboratory Animals and the Michelson Found Animals Foundation's Policy for Animals Involved in Research, and were approved by Iowa State University IACUC. All animals were at least eight weeks of age. The number of animals per group was determined by a statistical model based on prior studies with polyanhydride nanoparti-

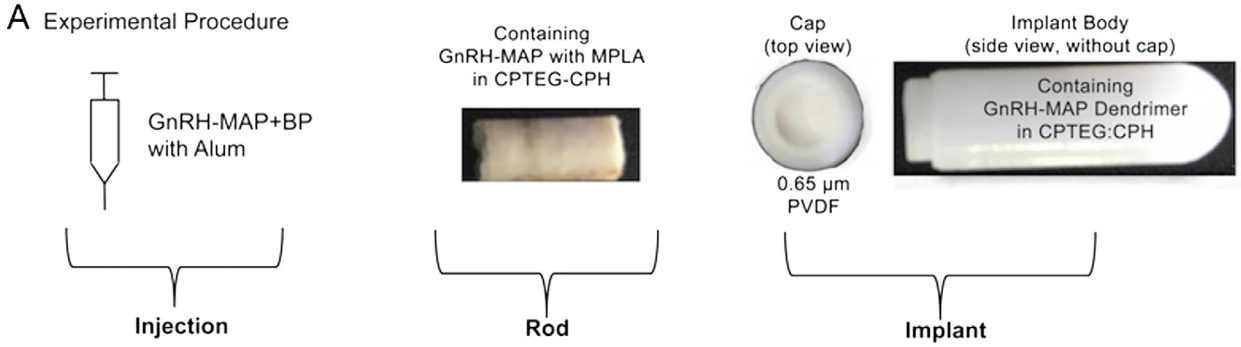

B Experimental Groups

	Injection	Rod	Implant
Group 1	X	X	X
Group 2	X		X
Group 3	X	X	
Group 4		X	X
Group 5			X
Group 6		X	
Group 7	Adjuvant Only		
Group 8	X		

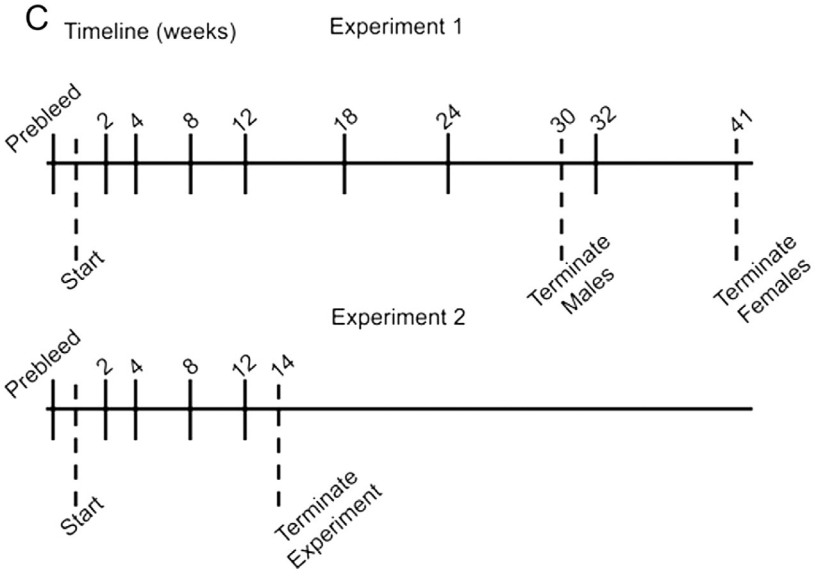

Fig. 1. Experimental design. (A) Schematic of the 3 stage platform. (B) Experimental groups 1–6 for experiment 1 and groups 1–8 for experiment 2. (C) Bleeding schedule for experiment 1 (top) and experiment 2 (bottom).

cles [30,31]. A 1 in. 27 gauge needle was used to inject the soluble vaccine caudal to the rod and implant. For implantation all animals weighed at least 20 g. Both the rod and implant were placed into subcutaneous tissue along the right side of the dorsum under general anesthesia with either an intraperitoneal injection of ketamine (100 mg/kg) and xylazine (10 mg/kg) for experiment 1 and experiment 2 males, or isofluorane inhalant anesthesia for experiment 2 females. The different experimental groups are outlined in Fig. 1B. Some animals required topical medication and/or cage separation to promote healing post-implantation. Animals were bled via the saphenous vein using manual restraint in accordance with the schedule shown in Fig. 1C.

2.7. Fluorescent GnRH ELISA

GnRH antibody determination was assayed via ELISA at 1:200 serum dilution in duplicate as described previously [32]. Briefly, biotinylated-GnRH peptide (BioSynthesis) was added at 17.5 pmol per well in PBS to NeutrAvidin™-coated BSA-blocked Black Plates (Thermo Scientific). Plates were incubated with polyclonal anti-mouse IgG F(ab')2-HRP (Thermo Scientific), washed, developed with Amplex® UltraRed Reagent, and stopped with Amplex® Red Stop Solution following manufacturer's instructions (Thermo Scientific).

2.8. Avidity index

Antibody avidity was assayed via as previously described [33]. Briefly, plates were coated with 5 µg/mL purified GnRH-MAP, incubated at 1:200 serum dilution, samples were treated with a serial dilution of 6.0 M sodium thiocyanate (Sigma Aldrich) in duplicate and developed with anti-mouse-HRP (Thermo Scientific) and Ultra-TMB (Thermo Scientific) substrate as directed by the manufacturer.

2.9. Cytokine assay

For *in vitro* antigen-recall cytokine responses, single cell suspensions of splenocytes were cultured in duplicate and supernatants were harvested 5 days post-stimulation as previously described [34]. IFN-γ, IL-5, and IL-10 levels were measured using a multiplexed magnetic bead assay (Luminex, Austin, TX) using a standard curve created with commercial cytokines per manufacturer's instruction.

2.10. Tissue collection and histology

At the time of euthanasia, testicles were excised and measured with calipers for length and width to estimate testicular volume and then placed in Davidson's fixative. Skin at the implantation site, ovaries and uterine tissue were harvested and placed into 10% neutral buffered formalin. Tissues were embedded in paraffin and processed into 10 µm tissue sections and stained with hematoxylin/eosin as previously described [35]. A board certified veterinary pathologist (Hostetter) was blinded to the experimental groups and assessed all sections of implant sites and/or rods for inflammation, macrophages, lymphocytes and plasma cells as well

as uterine histology. Uterine tissue was determined as *diestrus* with low cuboidal epithelium, few mitosis in epithelium, condensed stroma, no dilation, or *proestrus* with dilation of the uterine lumen, moderate mitoses and neutrophils, or *estrus* with tall cuboidal epithelium, numerous mitosis and low neutrophils, or *metestrus* with epithelial degeneration and low mitosis [36]. Testes and epididymis were assessed for mature sperm. Ovaries were scored for number of corpus luteum (CL)'s, degenerating CL's, and primary, secondary or tertiary follicles and cysts per tissue section.

2.11. Statistics

Standard ANOVA approaches with the Tukey or Bonferroni correction were used as indicated. Analysis of covariance was employed for the avidity index assay [37]. Log ratios = log(Y/X) where Y is antibody fluorescence at the experimental endpoint and X is antibody fluorescence at week 0. If Y/X = 1 then log(Y/X) = 0. A non-zero log ratio indicates detectable antibodies [38].

3. Results

3.1. Vaccine device

A 12 week dose response study (Supplementary Fig. 1) and a study with Alum and MPLA adjuvants (Supplementary Fig. 2) indicated that high doses of between 100 μg and 500 μg of GnRH-MAP linked to BP in Alum generated the highest antibody levels and MPLA as an adjuvant with 300 μg GnRH-MAP alone enhanced cell-mediated immunity and further reduced testicular size and altered expression of luteinizing hormone receptor (LHR) protein and insulin-like factor 3 (*Insl3*) mRNA, two molecules regulated by testosterone [39–41]. Although sterility was not achieved in male or female mice in this short time frame (data not shown) the studies defined the antigens and adjuvants for the vaccine platform design.

The vaccine platform consisted of three independent parts; a soluble injection of 300 μg GnRH-MAP-BP with alum (Sol); a 20:80 CPTEG:CPH PA-rod containing 300 μg GnRH-MAP and MPLA with all surfaces exposed to tissue (Rod); a cytoexclusive diffusion barrier implant containing 450 μg GnRH-MAP linked to a 8 arm PEG dendrimer in a 20:80 PA-rod limiting degradation to 1 surface (Implant, Fig. 1A). In experiment 1 there were six experimental groups (groups 1–6) with 4 male and 4 female mice per group (Fig. 1B). In the first experiment the implant was well-tolerated although five male mice lost their implants (out of 16 implants) randomly over the course of seven months (Table 1). These animals would present with the PVDF membrane end of the device exposed through the skin surface, or the device removed from the animal. Only one animal was terminated because of exposure of a polyanhydride rod, which became exposed within two weeks. All group 2 males lost their implants by seven months (30 weeks) prompting termination of the experiment. Female mice tolerated the implants extremely well for 10 months (38 weeks) when four animals from three different groups lost their implant. This experiment was terminated at 41 weeks.

We repeated these experiments adding two control groups (Fig. 1B, groups 1–8). Female mice tolerated the implants for two months when 40% of the implants (8 out of 20) were lost through weeks 8–10. All of the female mice, whether in the first or second experiment, lost their implants over the same four-week period. Males lost four implants of which only two were lost during the same weeks. This second experiment was terminated at 14 weeks, in part due to the loss of implants.

Gross examination of the implant sites showed that all PA-rods and implants were imbedded in subcutaneous fat with vessels visibly infiltrating the area around the PA-rod and implant cap. All implants had an intact PVDF membrane and the cap had a visible tissue interface that varied in color from red to white (Figs. 2A–C; Supplementary Fig. 3). The persistence of the collagen diffusion barrier within the implant varied, with experiment 1 males having the lowest success rate (estimated to be <30% with collagen present) and the females having the highest success rate (75% with collagen present). In the second experiment collagen was present in 50% of the implants of females and 40% of males. If no collagen was visible the barrier space was full of cell free straw colored clear fluid. One male from experiment 2 group 7 had thick white purulent material at the implant site.

3.2. Histology

Sections of haired skin, panniculus, and skeletal muscle from the PA-rod and/or implant site from both experiments were fixed for examination. In multiple sections PA-rods were present in the panniculus accompanied by mild to marked inflammatory cell infiltrates. The PA-rod was acellular amphophilic to eosinophilic fibrillary material that was often fragmented (Fig. 2E). The PA-rods were typically bordered by moderate to large numbers of macrophages enmeshed in immature fibrous connective tissue. There were occasional small to medium lymphoid aggregates that bordered the PA-rod or that were in the adipose tissue adjacent to the PA-rod (Fig. 2D, E). Low numbers of plasma cells and low to moderate numbers of neutrophils were occasionally seen in the subcutis around the PA-rod. In some sections there were well-delineated round to oval foci of fibrous tissue and macrophage aggregates that were often associated with a distinct clear space (presumed implant space). In these foci there was moderate fibrosis immediately around the clear space that was bordered by moderate to large numbers of macrophages with foamy, amphophilic to basophilic granular cytoplasm. There were multiple foci of neovascularization with thin wall endothelial lined capillaries or lymphatics within and adjacent to foci of fibrosis (Fig. 2F, G).

There were no differences in testicular size between any groups in either experiment 1 or 2 (data not shown) and mature sperm was found in the epididymis from all male mice (data not shown). All treatment groups had some ovulating female mice with no significant differences in ovarian structures such as CL's, degenerating CL's, and follicles (data not shown). Histological sections of the uteri of female mice in experiment 1 showed that animals were cycling with only group 2 having all animals in either diestrus or proestrus (Table 2, Fig. 3). The uterus was distended with fluid in 14 out of 24 animals in experiment 1 with groups 2, 4, and 6 most severely affected and group 3 having two animals with a purulent endometritis (Table 2). Female mice in experiment 2 were not scored for uterine changes.

3.3. Antibody levels and recall responses

ELISA results show anti-GnRH antibody levels at 1:200 serum dilution for experiment 1 females (Fig. 4A) and males (Fig. 4B) for all experimental groups over time. Using the log ratio of the wavelength at the last week versus the prebleed timepoint shows that all females with an implant, excluding the implant alone, had antibodies at 10 months post-vaccination (groups 1, 2, and 4). Group 1 was significantly higher than all other groups at week 41 (one-way ANOVA with Bonferroni correction). All males had detectable anti-GnRH antibodies with group 1 having highest levels at week 30 (one-way ANOVA with Bonferroni correction). The dynamic-predicted log ratio plots over time for each group are shown in Supplementary Fig. 4. Avidity index curves for antibodies from group 1 females and males show significantly enhanced antibody avidity at 41 and 30 weeks, respectively ($p < .001$, analysis of covariance) (Fig. 4C). Spleen cells isolated at the

Table 1
Implants lost.

Experiment 1			Experiment 2		
Group	Sex	Time post vaccine (weeks)	Group	Sex	Time post vaccine (weeks)
2	***Male***	***16***	1	Male	10
2	***Male***	***23***	***2***	***Male***	***3***
2	Male	Unknown	2	Male	8
2	Male	30	***4***	***Male***	***1***
3	***Male***	***1.5***	1	Female	8
4	***Male***	***10***	1	Female	9
1	Female	38	1	Female	11
2	Female	38	4	Female	8
4	Female	38	4	Female	9
4	Female	38	4	Female	11
			5	Female	Unknown
			7	Female	9
			7	***Female***	***1***

Exp. 1 termination 41 week; Exp. 2 termination week 14, Italics/bold = animal euthanized.

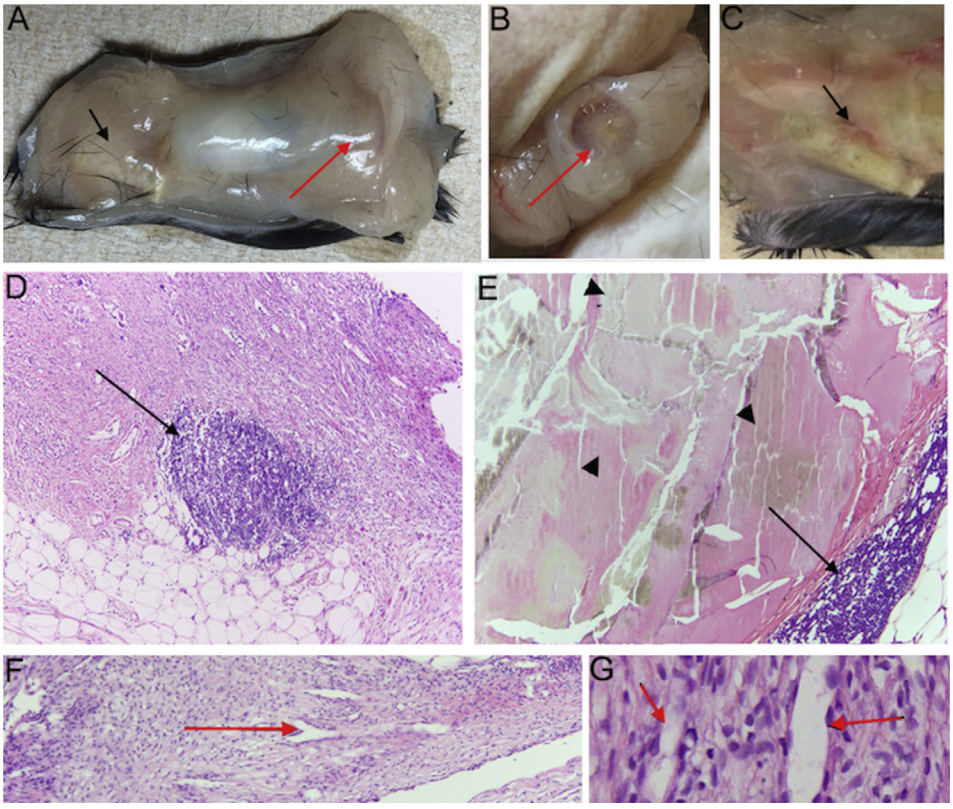

Fig. 2. Representative images of the implant and rod at 10 months post-vaccination in female mice. (A) Implant (red arrow), rod (black arrow) are visible in subcutaneous tissue. (B) The PVDF end of the implant. (C) Closer image of rod. (D-G) Representative histology of the site of implant and/or rod with lymphocytic aggregates (black arrows), PA (arrow heads) and blood vessels (red arrows). (For interpretation of the references to color in this figure legend, the reader is referred to the web version of this article.)

termination of the experiments and restimulated with GnRH-MAP showed significant increases in IFN-γ ($p = .0056$) and IL-5 ($p = .0158$) for females with no group being significantly different. Males had a significant increase only in IFN-γ ($p = .0056$). There were no significant increases in IL-10 for either males or females (Fig. 4D, E). For experiment 2, antibody levels were measured by ELISA at the termination of the experiment at 14 weeks post-vaccination. There were no significant differences between groups for females (one-way ANOVA with Tukey correction) whereas in males both groups 1 and 3 were significantly different than group 7 ($p = .0028$ one-way ANOVA with Tukey correction) (Supplementary Fig. 4).

4. Discussion

We sought to develop a vaccine device designed to mimic the principles of concomitant immunity in which infection by a pathogen maintains protective immunity within the host via dynamic antigen persistence [3,42,43]. In pursuit of this goal we developed a three-stage vaccine platform designed to prime, boost and maintain immunity to GnRH-MAP after a single vaccination.

Several promising aspects of the three-stage vaccine platform were discovered. The rods were well-tolerated in both experiments with only one animal out of 72 animals losing the rod. Detectable antibodies in 14 out of 16 animals in group 6 (rod only) from both

Table 2
Reproductive status of females.

Group	#	Status	Lumen fluid
1	1	D	0
	2	E	1
	3	E	0
	4	E	3
2	1	P	0
	2	D	3
	3	D	3
	4	D	3
3	1	D	0
	2	P	2
	3	[a]	
	4	[a]	
4	1	D	0
	2	P	2
	3	E	3
	4	M	3
5	1	D	0
	2	M	0
	3	D	0
	4	D	2
6	1	D	3
	2	M	2
	3	E	2
	4	P	3

D = diestrus, E = estrus, P = proestrus, M = metestrus. Reproductive status scoring rubric in materials and methods. 0 = no fluid, 1 = slight dilation, 2 = low # distended segments (<3/uterus), 3 = diffuse distension,
[a] =Purulent endometritis.

experiments indicates that (1) GnRH-MAP maintains immunogenicity after being formulated with PA and (2) sufficient immunogen is released from the rod with MPLA adjuvant to elicit an immune response in a majority of animals. Although at the termination of the experiments all PA-rods were grossly similar to their original size and shape (Fig. 2) degradation could be extensive with the overall shape of the PA-rod remaining unchanged [44–46], although future studies are needed. Overall the implants were tolerated moderately well except for a four-week period in which female mice in both experiments 1 and 2 lost 25% and 40% of the implants, respectively, whereas male mice lost 20–30% of their implants randomly over the course of the experiments (Table 1). It is reasonable to expect larger animals will have a significantly higher implant success rate. All implants assessed at the endpoint of experiment 1 or 2 had a grossly visible tissue interface formed on the PVDF membrane with macrophages, lymphocytic aggregates and neovascularization (Fig. 2). Although the fluid dynamics at the interface of the PVDF membrane is unknown, the space above the PA-rod was always fluid-filled or remained filled with collagen. Published studies of glucose transport in immune-isolation chambers indicate a dynamic relationship between fluids within implants and plasma for pore sizes as small as 10 nm [47]. In experiment 1, when the dynamics of the antibody response over the entire timecourse is compared between groups based on their predicted log ratios, group 2 (priming dose and implant) is different than group 3 (priming dose and rod) indicating that the implant design has a significant effect on the immune response that is different then that of the rod (Supplemental Fig. 5). Overall the components of the vaccine platform promoted effective priming, boosting and long-term maintenance of cell-mediated and antibody responses to an immunogen for up to 41 weeks with significant affinity maturation. Future studies are required to determine if antibody affinity is enhanced through any immune feedback mechanism [48,49].

The antibody levels in experiment 2 at the 14 week termination timepoint were inconsistent both within and between treatment groups. This could be a result of unknown inconsistencies generated during either the synthesis of the vaccine platform itself or its administration. Clearly the antibodies generated were not sufficient to promote sterility in mice in either experiment. This result suggests that higher antibody levels are warranted which could be addressed with different immunogen constructs or adjuvants. However, higher IL-10 levels in GnRH-MAP-BP vaccinated animals compared to BP only vaccinated animals (Supplemental Fig. 1) suggest that immunoregulatory mechanisms may limit the immune response to GnRH self-peptide and highlight another possible barrier in generating consistent long-term immunocastration using GnRH-based vaccines [50].

To generate and maintain immunity to a vaccine immunogen we designed a vaccine platform that would prime, boost and then maintain immunity with different antigen release mechanisms. To avoid tolerance and promote active immunity an immune feedback mechanism is proposed in which antibody levels could theoretically influence immunogen release by the formation of immune-complexes within a diffusion barrier between the vaccine depot and the implant opening. The vaccine platform is capable of maintaining both antigen-specific B cell and T cell responses for at least 10 months with a single dose. The sustained immunity generated with the vaccine platform supports further experiments to optimize antibody levels and/or determine the effectiveness of the current platform in other species, as well as determine if the vaccine platform is effective with a pathogen-specific vaccine. The vaccine platform is amenable to alternative designs and the immune response in different species could be targeted by adjusting the immunogen, dose, adjuvant, and release rates.

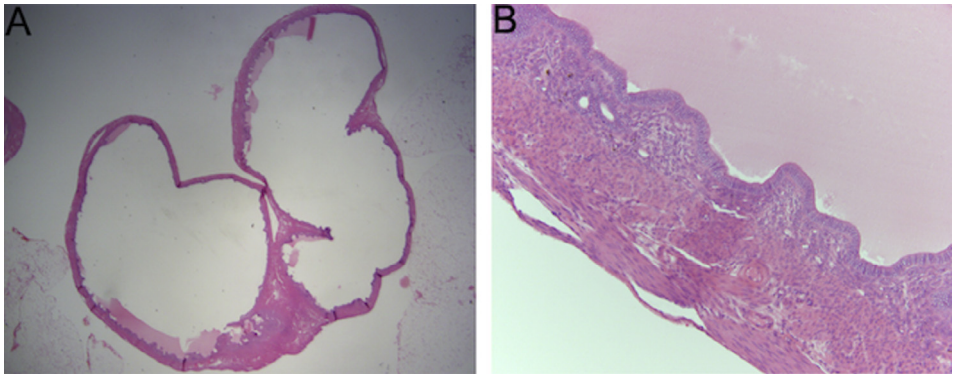

Fig. 3. Uterine histology with grade 3 distension (A) and estrus (B). A representative tissue section from a group 1 mouse at 10 months post-implantation. Scoring is described in materials and methods and Table 2.

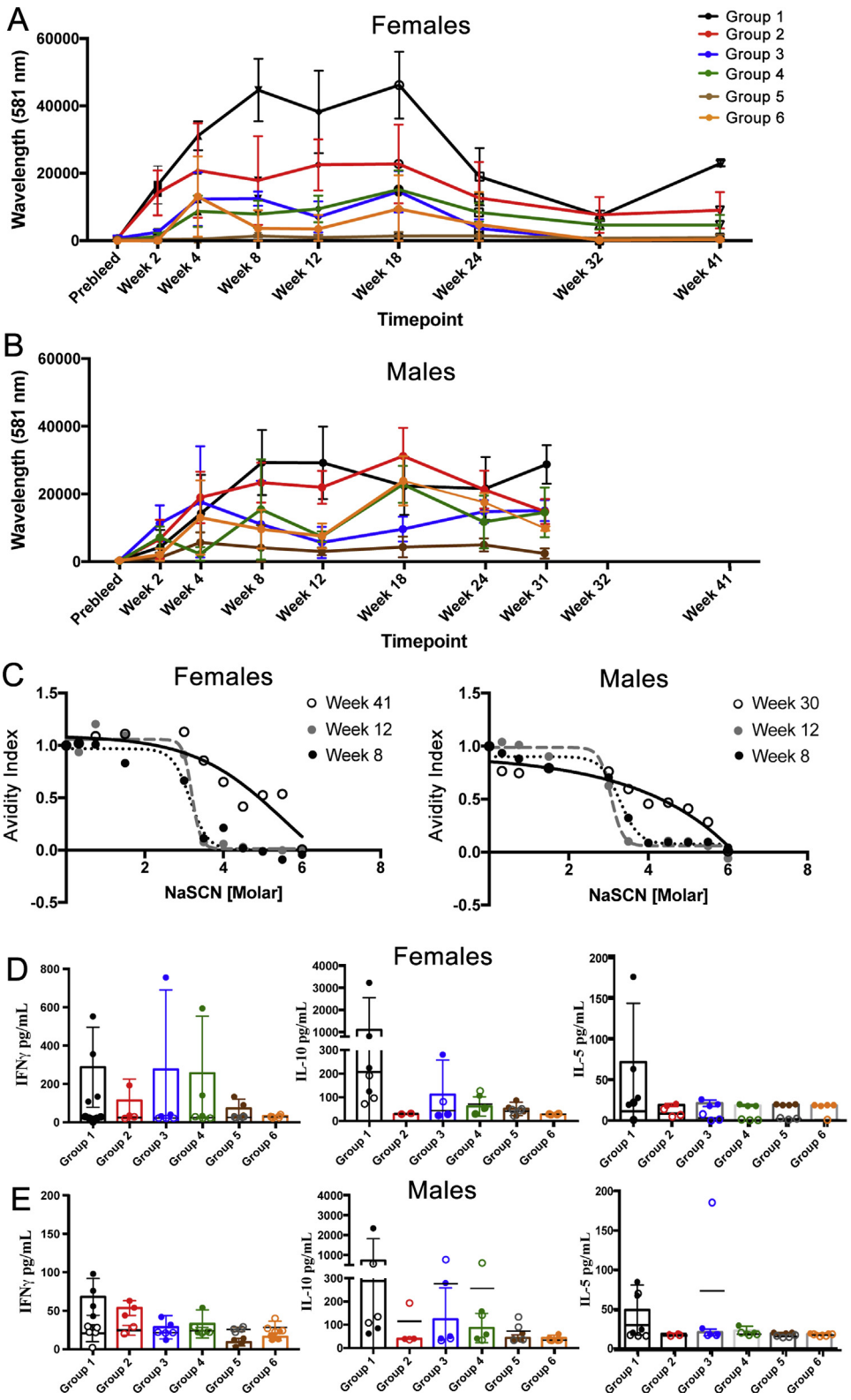

Fig. 4. Vaccine platform maintains antibody levels, recall responses and promotes enhanced avidity over time for animals in experiment 1. Anti-GnRH levels of (A) female mice and (B) males at time points indicated at serum dilution of 1:200. Mean ±SD. (C) Avidity index for antibodies from group 1 female (left) and male (right) mice at the indicated weeks post-vaccination. Each circle represents mean of 4 animals. (D and E) Cytokine levels, as indicated, from recall responses of spleen cells stimulated with GnRH-MAP for females (D) and males (E). Bars are mean of stimulated group ±std. dev. Each closed circle represents an individual animal. Open symbols are unstimulated levels.

Acknowledgements

This work was supported with a grant from the Michelson Prize & Grants, a program of the Michelson Found Animals Foundation, which is supported by the Generous Contributions of Dr. Gary Michelson and Alya Michelson. Support was also provided by an Iowa State University Bailey Award. The Vaccine Delivery Device and related claims are covered in U.S. patent application #14/814148 (Jones, Brewer, Narasimhan, Jackman).

Conflict of Interest

The authors have no conflicts of interest to disclose.

Appendix A. Supplementary material

Supplementary data associated with this article can be found, in the online version, at https://doi.org/10.1016/j.vaccine.2017.12.050.

References

[1] Brown SP, Grenfell BT. An unlikely partnership: parasites, concomitant immunity and host defence. Procee Biol Sci 2001;268:2543–9.
[2] Mandell MA, Beverley SM. Continual renewal and replication of persistent *Leishmania major* parasites in concomitantly immune hosts. Proc Natl Acad Sci USA 2017;114:E801–10.
[3] Peters NC, Pagan AJ, Lawyer PG, Hand TW, Henrique Roma E, Stamper LW, et al. Chronic parasitic infection maintains high frequencies of short-lived Ly6C$^+$CD4$^+$ effector T cells that are required for protection against re-infection. PLoS Pathog 2014;10:e1004538.
[4] Wikler M, Pearson LK, Campbell AJ, Tibary A. Non-surgical methods of contraception and sterilization in select domestic and wildlife species. Clin Theriogenol 2014;6:93–104.
[5] Ferro VA, Costa R, Carter KC, Harvey MJ, Waterston MM, Mullen AB, et al. Immune responses to a GnRH-based anti-fertility immunogen, induced by different adjuvants and subsequent effect on vaccine efficacy. Vaccine 2004;22:1024–31.
[6] Levy JK, Friary JA, Miller LA, Tucker SJ, Fagerstone KA. Long-term fertility control in female cats with GonaCon, a GnRH immunocontraceptive. Theriogenology 2011;76:1517–25.
[7] Benka VA, Levy JK. Vaccines for feline contraception: GonaCon GnRH-hemocyanin conjugate immunocontraceptive. J Feline Med Surg 2015;17:758–65.
[8] Miller LA, Fagerstone KA, Eckery DC. Twenty years of immunocontraceptive research: lessons learned. J Zoo Wildl Med 2013;44:S84–96.
[9] Naz RK, Saver AE. Immunocontraception for Animals: current Status and Future Perspective. Am, J Reprod Immunol 2016.
[10] Torres MP, Vogel BM, Narasimhan B, Mallapragada SK. Synthesis and characterization of novel polyanhydrides with tailored erosion mechanisms. J Biomed Mater Res Part A 2006;76:102–10.
[11] Ross KA, Loyd H, Wu W, Huntimer L, Ahmed S, Sambol A, et al. Hemagglutinin-based polyanhydride nanovaccines against H5N1 influenza elicit protective virus neutralizing titers and cell-mediated immunity. Int J Nanomed 2015;10:229–43.
[12] Ulery BD, Kumar D, Ramer-Tait AE, Metzger DW, Wannemuehler MJ, Narasimhan B. Design of a protective single-dose intranasal nanoparticle-based vaccine platform for respiratory infectious diseases. PloS One 2011;6:e17642.
[13] Petersen LK, Xue L, Wannemuehler MJ, Rajan K, Narasimhan B. The simultaneous effect of polymer chemistry and device geometry on the in vitro activation of murine dendritic cells. Biomaterials 2009;30:5131–42.
[14] Carrillo-Conde B, Song EH, Chavez-Santoscoy A, Phanse Y, Ramer-Tait AE, Pohl NL, et al. Mannose-functionalized pathogen-like polyanhydride nanoparticles target C-type lectin receptors on dendritic cells. Molecular Pharm 2011;8:1877–86.
[15] Vela-Ramirez JE, Goodman JT, Boggiatto PM, Roychoudhury R, Pohl NL, Hostetter JM, et al. Safety and biocompatibility of carbohydrate-functionalized polyanhydride nanoparticles. AAPS J 2015;17:256–67.
[16] Petersen LK, Huntimer L, Walz K, Ramer-Tait A, Wannemuehler MJ, Narasimhan B. Combinatorial evaluation of in vivo distribution of polyanhydride particle-based platforms for vaccine delivery. Int J Nanomed 2013;8:2213–25.
[17] Kipper MJ, Wilson JH, Wannemuehler MJ, Narasimhan B. Single dose vaccine based on biodegradable polyanhydride microspheres can modulate immune response mechanism. J Biomed Med Res 2006;76A:798–810.
[18] Wafa EI, Geary SM, Goodman JT, Narasimhan B, Salem AK. The effect of polyanhydride chemistry in particle-based cancer vaccines on the magnitude of the anti-tumor immune response. Acta Biomaterialia 2017;50:417–27.
[19] Haughney SL, Ross KA, Boggiatto PM, Wannemuehler MJ, Narasimhan B. Effect of nanovaccine chemistry on humoral immune response kinetics and maturation. Nanoscale 2014;6:13770–8.
[20] Coffman RL, Sher A, Seder RA. Vaccine adjuvants: putting innate immunity to work. Immunity 2010;33:492–503.
[21] Jain RK, Stylianopoulos T. Delivering nanomedicine to solid tumors. Nature Rev Clin Oncol 2010;7:653–64.
[22] Teuscher C, Donaldson DM. The deposition and formation of immune complexes in collagenous tissues. Clin Immunol Immunopathol 1979;13:56–66.
[23] Jasin HE. Mechanism of trapping of immune complexes in joint collagenous tissues. Clin Exp Immunol 1975;22:473–85.
[24] Wallace DG, Rosenblatt J. Collagen gel systems for sustained delivery and tissue engineering. Adv Drug Deliv Rev 2003;55:1631–49.
[25] Schaut RG, Brewer MT, Mendoza K, Jackman J, Narasimhan B, Jones DE. A polyanhydride-based implantable single dose vaccine platform for long-term immunity. Vaccine 2017.
[26] Beekman NJ, Schaaper WM, Turkstra JA, Meloen RH. Highly immunogenic and fully synthetic peptide-carrier constructs targetting GnRH. Vaccine 1999;17:2043–50.
[27] Miller LA, Gionfriddo JP, Fagerstone KA, Rhyan JC, Killian GJ. The single-shot GnRH immunocontraceptive vaccine (GonaCon) in white-tailed deer: comparison of several GnRH preparations. Am J Reprod Immunol. 2008;60:214–23.
[28] Kipper MJ, Narasimhan B. Molecular description of erosion phenomena in biodegradable polymers. Macromolecules 2005;38:1989–99.
[29] Pieper JS, Hafmans T, Veerkamp JH, van Kuppevelt TH. Development of tailor-made collagen-glycosaminoglycan matrices: EDC/NHS crosslinking, and ultrastructural aspects. Biomaterials 2000;21:581–93.
[30] Joshi VB, Geary SM, Carrillo-Conde BR, Narasimhan B, Salem AK. Characterizing the antitumor response in mice treated with antigen-loaded polyanhydride microparticles. Acta Biomater 2013;9:5583–9.
[31] Huntimer L, Wilson Welder JH, Ross K, Carrillo-Conde B, Pruisner L, Wang C, et al. Single immunization with a suboptimal antigen dose encapsulated into polyanhydride microparticles promotes high titer and avid antibody responses. J Biomed Mater Res Part B, Appl Biomater 2013;101:91–8.
[32] Li J, Olvera AI, Akbari OS, Moradian A, Sweredoski MJ, Hess S, et al. Vectored antibody gene delivery mediates long-term contraception. Curr Biol 2015;25:R820–2.
[33] Pullen GR, Fitzgerald MG, Hosking CS. Antibody avidity determination by ELISA using thiocyanate elution. J Immunol Methods 1986;86:83–7.
[34] Osanya A, Song EH, Metz K, Shimak RM, Boggiatto PM, Huffman E, et al. Pathogen-derived oligosaccharides improve innate immune response to intracellular parasite infection. Am J Pathol 2011;179:1329–37.
[35] Gibson-Corley KN, Boggiatto PM, Bockenstedt MM, Petersen CA, Waldschmidt TJ, Jones DE. Promotion of a functional B cell germinal center response after *Leishmania* species co-infection is associated with lesion resolution. Am J Pathol 2012;180:2009–17.
[36] Comparative anatomy and histology: a Mouse and Human Atlas 2011.
[37] Montgomery DC. Design and Analysis of Experiments. 8th ed. John Wiley & Sons, Incorporated; 2012.
[38] Ramsay JO, Hooker G, Graves S. Functional Data Analysis with R and MATLAB. New York: Springer; 2009.
[39] Roth MY, Lin K, Bay K, Amory JK, Anawalt BD, Matsumoto AM, et al. Serum insulin-like factor 3 is highly correlated with intratesticular testosterone in normal men with acute, experimental gonadotropin deficiency stimulated with low-dose human chorionic gonadotropin: a randomized, controlled trial. Fertility Sterility 2013;99:132–9.
[40] Ivell R, Heng K, Anand-Ivell R. Insulin-Like Factor 3 and the HPG Axis in the Male. Front Endocrinol 2014;5:6.
[41] Ivell R, Wade JD, Anand-Ivell R. INSL3 as a biomarker of Leydig cell functionality. Biol Reprod 2013;88:147.
[42] Vanloubbeeck Y, Jones DE. Protection of C3HeB/FeJ mice against *Leishmania amazonensis* challenge after previous *Leishmania major* infection. Am J Trop Med Hyg 2004;71:407–11.
[43] Doolan DL, Dobano C, Baird JK. Acquired immunity to malaria. Clin Microbiol Rev 2009;22:13–36.
[44] Tabata Y, Gutta S, Langer R. Controlled delivery systems for proteins using polyanhydride microspheres. Pharm Res 1993;10:487–96.
[45] Mathiowitz E, Kline D, Langer R. Morphology of polyanhydride microsphere delivery systems. Scanning Microscopy 1990;4:329–40.
[46] Laurencin CT, Gerhart T, Witschger P, Satcher R, Domb A, Rosenberg AE, et al. Bioerodible polyanhydrides for antibiotic drug delivery: in vivo osteomyelitis treatment in a rat model system. J Ortho Res: Official Publication Ortho Res Soc 1993;11:256–62.
[47] Leoni L, Desai TA. Nanoporous biocapsules for the encapsulation of insulinoma cells: biotransport and biocompatibility considerations. IEEE Trans Bio-med Eng 2001;48:1335–41.
[48] Tas JM, Mesin L, Pasqual G, Targ S, Jacobsen JT, Mano YM, et al. Visualizing antibody affinity maturation in germinal centers. Science 2016;351:1048–54.
[49] Mesin L, Ersching J, Victora GD. Germinal Center B Cell Dynamics. Immunity 2016;45:471–82.
[50] Strasser A, May B, Teltscher A, Wistrela E, Niedermuller H. Immune modulation following immunization with polyvalent vaccines in dogs. Vet Immunol Immunopathol 2003;94:113–21.